International Symposium on Solar Physics and Solar Eclipses (SPSE) 2006
R. Ramelli, O. M. Shalabiea, I. Saleh, and J.O. Stenflo, eds.

USING POLARIMETRIC IMAGING AND SPECTROSCOPY OF THE CORONA FROM 400 TO 1800 NM FOR EXPLORING THE NEAR SUN PLASMA

SHADIA RIFAI HABBAL, JEFF KUHN, DONALD MICKEY, SARAH JAEGGLI, HUW MORGAN and ILIA ROUSSEV
Institute for Astronomy, University of Hawaii, Honolulu, HI 96822, USA

JUDD JOHNSON
Electricon, Boulder, CO 80204, USA

MARTINA BELZ ARNDT
Department of Physics, Bridgewater State College, Bridgewater, MA 02325, USA

ADRIAN DAW
Department of Physics and Astronomy, Appalachian State University, Boone, NC 28608, USA

and

MUNIR H. NAYFEH
Department of Physics, University of Illinois at Urbana-Champaign, IL 61801, USA

Abstract. Total solar eclipses offer unique opportunities for exploring the solar corona, in particular for validating new concepts, and testing new instrumentation. The scientific goals of the experiments, planned for the total solar eclipse of 29 March 2006, at Waw AnNamous, Libya, by the eclipse group from the Institute for Astronomy (IfA) at the University of Hawaii, were as follows: (1) to search for the signature of silicon nanometer size dust grains in the corona, (2) to search for the signature of a neutral wind of interstellar origin in the corona, (3) to understand the nature of near-Sun dust from F-coronal visible and IR spectra, and (4) to establish the direction of the coronal magnetic field from its origin at the Sun as it expands into interplanetary space. A complement of imaging and spectroscopic polarization measurements, covering the wavelength range from 400 to 1800 nm, were designed and constructed to achieve these objectives. The observing conditions during the total solar eclipse deemed ideal, and the experiments were successfully executed to achieve these milestones.

Key words: solar corona, infrared emission, polarization, interplanetary dust, magnetic fields

1. Introduction

A number of novel concepts regarding the composition of the solar corona have recently emerged from coronal observations made in the near-infrared part of the solar spectrum during total solar eclipses.

In their eclipse observations of 21 June 2001, Habbal *et al.* (2003) found a tangentially polarized emission within the 0.5 nm bandpass of the Fe XIII 1074.7 nm filter. This errant polarization appeared in low-temperature and low-density regions of the corona, such as coronal holes, where this emission should have been absent. This was in contrast to the predominantly radial polarization direction observed in

the rest of the corona. This tangential polarization could not be accounted for by the theory of radiative excitation of coronal forbidden lines, such as the Fe XIII line (Charvin, 1965). In addition, the radial profile of the Fe XIII intensity as a function of radial distance, in the coronal regions with tangential polarization, dropped sharply close to the Sun, as expected from collisional excitation, but then flattened considerably when compared to the emission in the continuum (see Figure 1a).

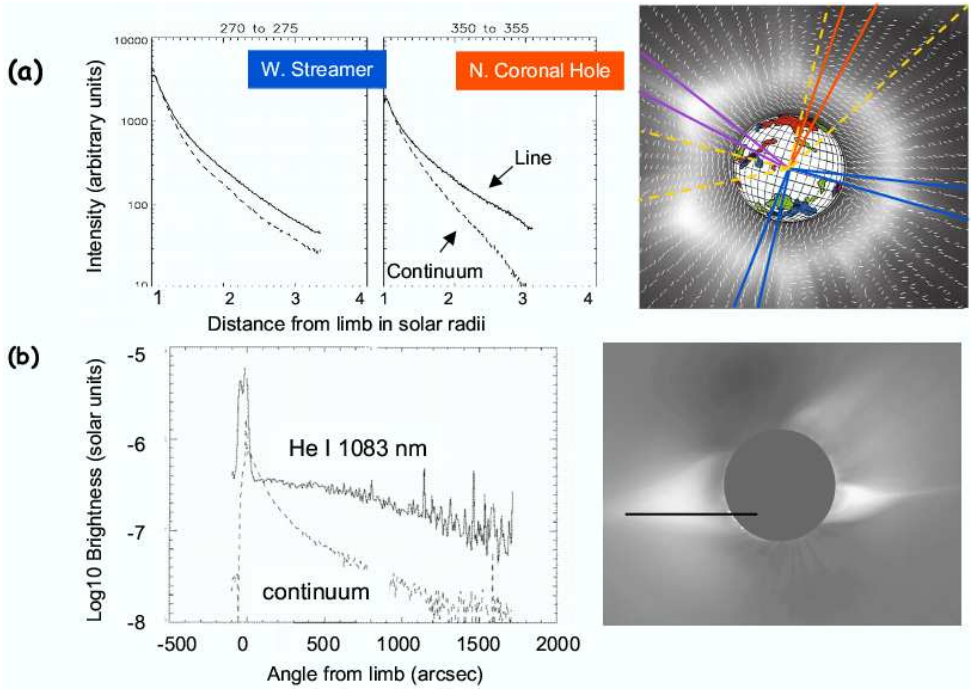

Fig. 1. Composite from the eclipse observations of (a) 2001 by Habbal et al. (2003) and (b) 1994 by Kuhn et al. (1996). (a) Radial profiles of the intensity of the Fe XIII 1074.7 nm line and neighboring continuum in arbitrary count units, versus radial distance, within 5 deg swaths given by the position angles above each panel. (The position angle is measured counter-clockwise from 0 degrees north). To the right is a map of the polarization angle for the 1074.7 nm Fe XIII line superimposed on the white-light image of the corona taken at the same time. The thick lines outline different regions in the corona where radial profiles of the intensity were plotted. (b) Radial profile of the He I 1083 nm line intensity compared to the continuum. To its right is the white light image of the corona with the spectrograph slit position and extent given by the straight line.

Taken together, the unexpected polarization direction and radial fall-off of line intensity were attributed to fluorescence from silicon nanometer dust grains in the inner corona. The assertion was based on observations in the interstellar medium (see, e.g. Witt *et al.*, 1998; Nayfeh *et al.*, 2005,) and on recent laboratory experiments by M. Nayfeh and his group (Nayfeh *et al.*, 2001; Belomoin *et al.*, 2002) who discovered silicon nanoparticle distributions in discrete and reproducible family of sizes, with diameters of 1, 1.67, 2.15, 2.9 and 3.7 nm. These particles become highly fluorescent in the visible, red, and infrared part of the spectrum under UV radiation. If present in the corona, the observed tangential polarization could be an indication

that this absorption/fluorescence process is a consequence of changes in the internal structure of the nanoparticles as a result of vibrational and rotational modes triggered by UV excitation. This conjecture is further supported by model calculations (Mann *et al.*, 2000) indicating that the radiation pressure force for silicates 5–10 nm in size is smaller than the gravitational force, thus enabling nanometer-size dust grains to get very close to the Sun.

During the 1994 eclipse, Kuhn *et al.* (1996) reported the discovery and confirmation of the existence of a number of spectral lines in the near infrared part of the spectrum. In particular, the S IX emission at 1252.5 nm was detected, and the Si X emission at 1430 nm was confirmed. In addition, an extended emission was observed in the He I 1083 nm line of neutral helium, with a redshift increasing with heliocentric distance to approximately 20 km/s. As shown in the reproduction of Figure 1b, the slit of the spectrograph in that experiment coincided with a high density streamer. Close to the Sun, one end of the slit overlapped a prominence, and the slit extended to about 3 R_s outwards. Curiously, the decrease in the He I line intensity with radial distance resembled the behavior of the Fe XIII line radial profile in a coronal hole in the 2001 eclipse measurements, characterized by a sharp drop off very close to the Sun, followed by a shallow profile. Hence, in both cases, the unexpected shape of the radial profiles occurred in coronal regions where emission from either Fe XIII (2001 data) or He I (1994 data) should have been absent.

Recently, the He I emission in 1994 data has been attributed to the focussing of the interstellar neutral He wind in the corona by solar gravity. This interpretation was supported by recent observations made on 14 February 2005 (Kuhn et al. 2006) with the coronagraph on Haleakala (SOLARC), and by ultraviolet coronagraph observations in the extended corona by the UVCS instrument on SoHO (e.g., Michels *et al.*, 2002).

Given the importance of the near-infrared part of the spectrum, it behooved us to focus on this wavelength range to follow up on these novel earlier findings, and to exploit the diagnostic power of polarimetric imaging and spectroscopy of the corona during the total solar eclipse of 29 March 2006 at Waw AnNamous, Libya. In what follows we briefly describe the suite of eclipse experiments (section 2), and present preliminary results (section 3). We conclude in section 4.

2. The IfA/UH eclipse experiments

A suite of three sets of instruments were designed and constructed to carry out polarimetric imaging and spectroscopy of the corona from 400 to 1800 nm.

2.1. The Near-Infared Imaging Spectropolarimeter

The Near-Infrared Imaging Spectropolarimeter (NIIS) was designed for imaging spectroscopy of the corona, with coarse spatial resolution but relatively high spectral resolution, by measuring intensities of several coronal emission lines simultaneously. The instrument comprises five major optical components: a simple telescope, a linear polarizer, an optical fiber bundle, a grating spectrograph and a camera.

The telescope optics consists simply of a spherical mirror of 7.5 cm diameter, tilted to form an image of the corona to the side of the telescope entrance aperture.

At its focus is a hexagonal array of 127 optical fibers, spaced uniformly to sample the corona out to 4 R_s, with a spatial resolution of about 7.5 arc minutes. The telescope is defocused so that each fiber samples a region about equal to the spacing between fibers.

Placed in front of the fiber array is a linear polarizer which may be rotated under computer control. The polarizer was rotated 45° between exposures, so the polarization of the coronal light can be obtained from a combination of four exposures.

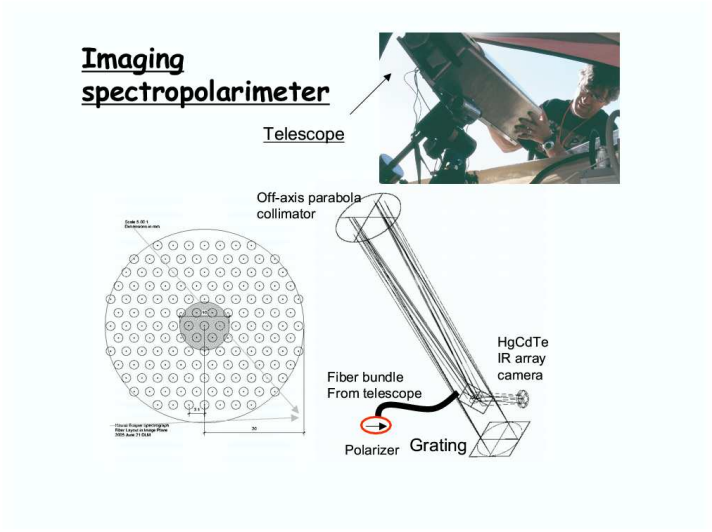

Fig. 2. The near-infrared imaging spectropolarimeter design, and a photo of the telescope part as mounted in the observing tent.

The optical fibers are rearranged at their output end into a linear array, with the fibers packed closely together. This linear array becomes the effective entrance slit of a Littrow-configuration reflecting grating spectrograph. The spectrograph produces a separate 2-pixel FWHM-wide spectrum from each fiber, with a resolving power of approximately 500. A 1024×1024 liquid nitrogen-cooled HgCdTe array camera is then used to record all 127 spectra simultaneously. The array was manufactured by Raytheon, Inc., and to our knowledge, is the first time these novel HgCdTe detectors have been used for solar astrophysics. A short-pass filter was used to limit thermal background at the detector and results in a useful wavelength range from 1 to 1.9 μm (See Figure 2).

2.2. The integrated visible wavelength spectrometer

A fiber optic spectrograph system was designed and built to measure the spatially integrated spectrum of a 2.5 R_s diameter annular region of the corona from 400 to 1100 nm. A spherical mirror focused the coronal light onto an annular fiber bundle, whose fibers were gathered and then illuminated the slit of an Ocean Optics

Spectrograph (see Figure 3). Simultaneous and co-aligned images of the corona were taken with a Sony video camera to follow the center of the field of view in the corona. The annular region over which light was spatially integrated was initially centered on the solar disk but also was repointed during totality to sample the outer F-corona at a distance of about 6 solar radii from disk-center.

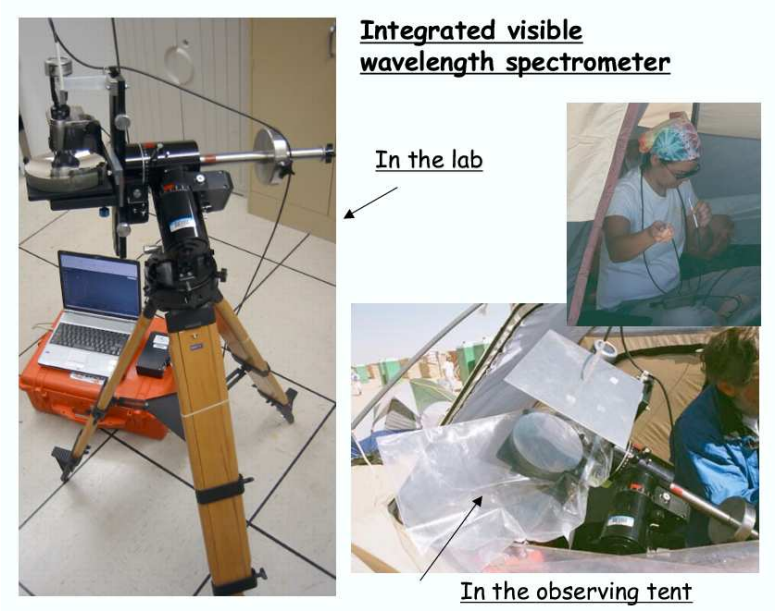

Fig. 3. The integrated visible wavelength spectrometer assembly in the lab (left), and in the eclipse observing tent (right).

2.3. The imaging polarimeter

Imaging of the corona was done simultaneously through three narrow (0.5nm) band-pass filters centered at 789.2, 1074.7 and 1083.0 nm, corresponding to the coronal emission lines of Fe XI, Fe XIII and He I respectively. In addition, a 50 nm wide filter, centered at 650 nm, was used for polarized brightness measurements of the white light coronal emission produced by electrons scattering photospheric radiation (see Figure 4). With the exception of the broadband filter, all filters were thermally controlled. Polarization measurements were made with all filters except 789.2. Each polarizer was rotated by 45° between exposures. Two identical electro-thermally cooled PIXIS 1024BR cameras, manufactured by Princeton Instruments, were used. They were both mounted on the same equatorial mount, each fitted with two filters that could be interchanged during the observations. The cameras have a 1024×1024 CCD array, with peak quantum efficiency of 87% at 800 nm, dropping down to 5% at 1100 nm. The polarizers were placed ahead of the filters, which were mounted on Nikon 300 mm focal length lenses. The observations were taken with 4 positions of the polarizer, separated by 45 degrees, at normal incidence, and with the filters tilted by 7° for observations in the nearby continuum. A number of exposure times,

Fig. 4. Two views of the imaging polarimeter from within the observing tent. Two PIXIS 1024BR cameras are mounted on the same German Equatorial mount, with filters attached to each camera. The filters could be interchanged during the observing run. The polarizers were manually controlled.

varying from a fraction of a second to 14 seconds, were used.

3. Preliminary Results

Shown in Figure 5 is an example from the IR spectrum taken with NIIS in the different fibers, hence at different spatial locations (i.e. latitude and radial distance) in the corona. The most dominant lines are those of Fe XIII 1074.7 nm and He I 1083 nm. The next dominant lines are the S IX emission at 1252.5 nm and Si X at 1430 nm. There is a new strong unidentified line around 1660 nm. In addition to the polarized spectrum, the other novel outcome of the NIIS measurements was a near-IR coronal image reconstructed from the polarized intensity collected by each fiber.

An example of a spectrum taken with the integrated visible wavelength spectrometer is shown in Figure 6. The spectrum was recorded when the fiber bundle was centered at the Sun, and is dominated by emission from the prominence off the east limb. A number of spectral lines are identified, and some are unknown. Note that the Fe XIII 1074.7 nm line is missing while the He I 1083 nm line is very prominent. This is a result of the reduced quantum efficiency of the detector around 1000 nm. However, the signal from the He I 1083 nm emission suggests that, despite the very low response of the detector at that wavelength, the intensity of the He I emission from the prominence was strong enough to be measurable, as opposed to the 1074.7 nm line that was not.

An example of the polarized brightness images taken in the broad band (pB) and at 1074.7 nm narrow bandpass filters are shown in Figure 7. Also shown is

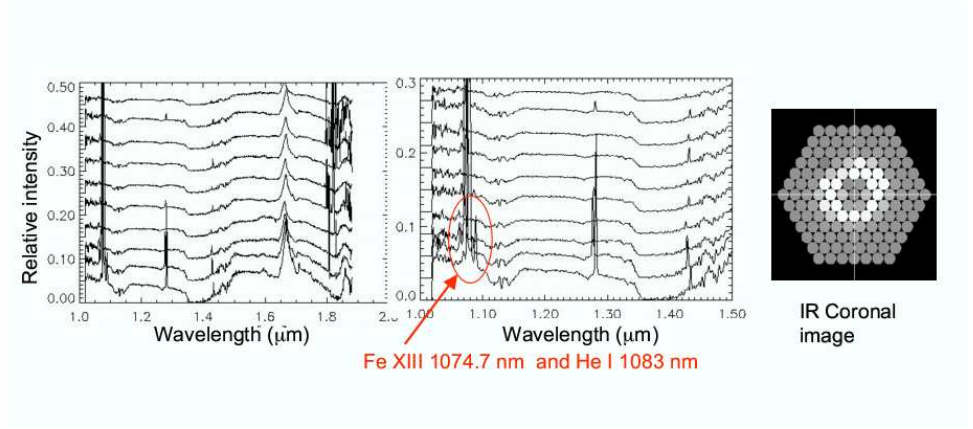

Fig. 5. Left: A sample near-IR spectrum covering 1-1.8 microns. The sample spectra collected from different fibers pointing at different regions of the corona, as shown in the IR coronal image to the right, are offset vertically in this plot. Middle: An enlargement of the left panel, with emphasis on the 1-1.5 micron wavelength range. The dominant emissions from the Fe XIII 1047.7 nm and He I 1083.0 nm lines are encircled. Right: A reconstructed image of the corona in the near IR from the integrated intensity in each fiber. Each circle represents the field of view of one fiber.

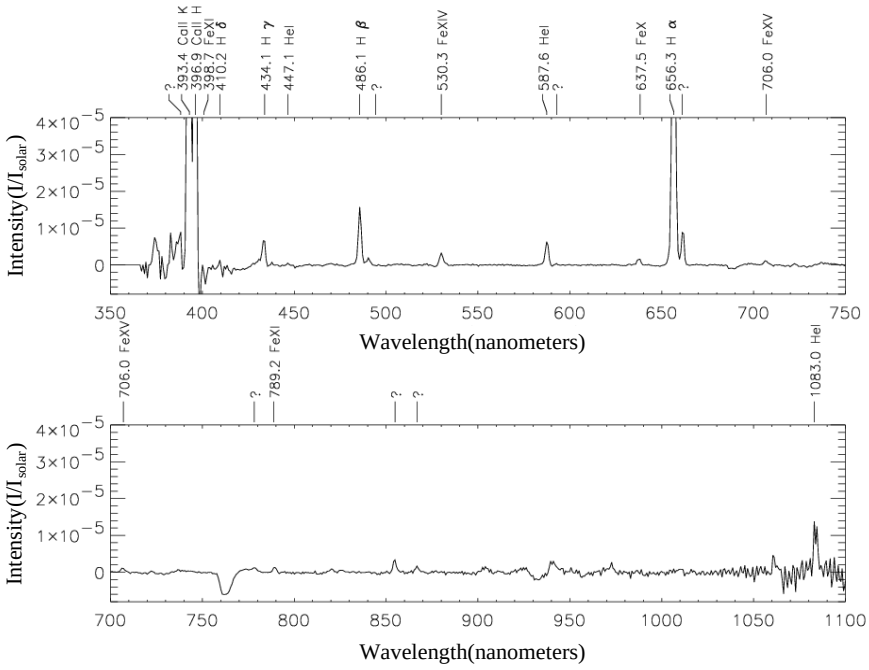

Fig. 6. An example of the *flattened* visible spectrum taken when the fiber bundle was centered at the Sun. The wavelength range covers 350–1100 nm. In this display the spectrum is divided equally in two parts with a repetition of the 700–750 nm range.

an image taken in Fe XI 789.2 nm which yielded a surprising result. The extent of the emission out to the edge of the field of view was quite unexpected, pointing to a dominance of the emission by resonant scattering beyond a fraction of a solar radius.

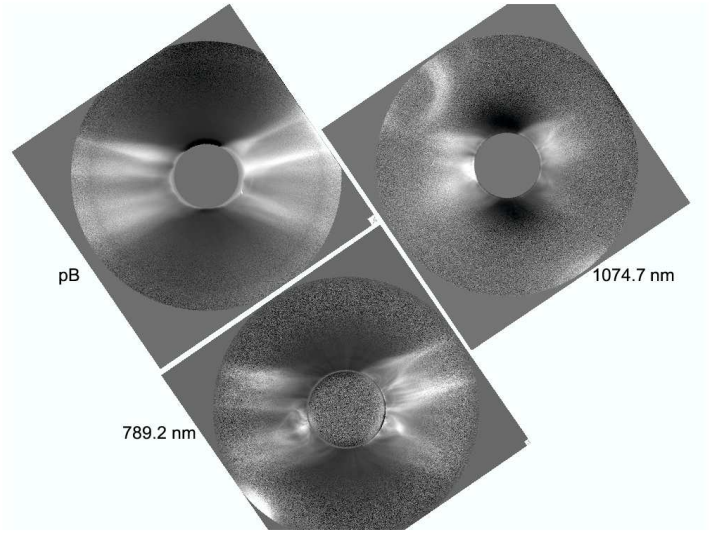

Fig. 7. Polarized brightness image (left) taken with the broadband filter centered at 650nm with a bandpass of 50 nm, polarized brightness image in 1074.7 nm (right) with a bandpass of 1 nm, and intensity image of the 789.2 nm Fe XI line (bottom panel). The orientation of the images is such that solar north is up.

4. Discussion and Conclusions

By all measures the eclipse observations made with the complement of three instruments were very successful. The results presented above are only preliminary, and data analysis is ongoing to answer the key questions that were the goal of the observations: (1) Can we detect and characterize a signature of nanometer size dust grains in the corona, (2) is there a neutral wind of interstellar origin in the corona, (3) can we characterize the near-Sun dust from F-coronal imaging and integrated visible spectroscopy, and (4) can we unambiguously identify the direction of the coronal magnetic field to place stringent constraints on theories of coronal expansion and solar wind acceleration? One totally unexpected result from these planned measurements, was the extended emission in the 789.2 nm Fe XI line, which has the potential to be a powerful diagnostic tool for future coronagraphic observations from both ground and space.

Acknowledgements. The members of the IfA eclipse group (see Figure 8) are grateful to Profs. Abdel Hamid Zeidan and Osama Shalabiea for their vision and relentless efforts that led to the

Fig. 8. Members of the IfA eclipse team at the observing site on 30 March 2006. Left to right, top row: Huw Morgan, Sarah Jaeggli, Judd Johnson, Shadia Habbal, Martina Arndt; bottom row: Adrian Daw, Jeff Kuhn, Ilia Roussev, and Don Mickey.

outstanding success of the eclipse observations at Waw AnNamous in Libya. We are also thankful to Abdel Razak Gherwash and Rob Schreuders for providing the necessary facilities at the eclipse camp site, in particular the liquid nitrogen and generators. We thank Alan Lichty from Princeton Instruments for enabling us to borrow a PIXIS near IR camera. We are also grateful to Diane Sakamato and Faye Uyehara for their help with instrument procurements and travel arrangements, to Lee Ann Scardina and Elizabeth Gutierrez, from DHL-USA, and Sayed Sabra and Mohammed AlSheybani, from DHL-Libya, for providing affordable and reliable shipping of the observing equipment to and from Libya, and to Appalachian State University Research Council for supporting the participation of A. Daw. Support for this project was provided by NSF grant ATM-0450799 to the Institute for Astronomy at the University of Hawaii.

References

Belomoin, G., *et al.*: 2002, *App. Phys. Lett.* **80**, 841
Charvin, P.: 1965, *Ann. d'Astrophys.* **28**, 877
Habbal, S. R., Arndt, M. B., Nayfeh, M. H., Arnaud, J., Johnson, J., Hegwer, S., Woo, R., Ene, A. and Habbal, F.: 2003, *ApJ*, **592**, L87
Kuhn, J. R., Jaeggli, S, Lin, H., and Arnaud, J.: 2006, COSPAR (in press)
Kuhn, J. R., Penn, M. J., and Mann, I.: 1996, *ApJ* **456**, L67
Mann, I., Krivov, A, and Kimura, H.: 2000, *Icarus* **146**, 568
Michels, J. G., *et al.* :2002, *ApJ* **568**, 385
Nayfeh, M. H. *et al.*: 2001, *Appl. Phys. Lett.* **78**, 1131
Nayfeh, M. H., Habbal, S. R., and Rao, S.: 2005, *ApJ* **621**, L121
Witt, A. N., Gordon, K., and Furton, D. G.: 1998, *ApJ* **501**, L111